

Laboratory Study

Regeneration of peritoneal mesothelium in a rat model of peritoneal fibrosis

Yoshiaki Nishioka*, Masanobu Miyazaki*, Katsushige Abe*, Akira Furusu*, Takashi Harada[¶], Yoshiyuki Ozono[§], Takashi Taguchi[†], Takehiko Koji[‡], Shigeru Kohno*

*Second Department of Internal Medicine, [¶]Division of Renal Care Unit,

[§]Department of General Medicine, [†]Second Department of Pathology, [‡]Department of Histology and Cell Biology, Nagasaki University School of Medicine, NAGASAKI, JAPAN

Running title: Regeneration of fibrotic peritoneal mesothelium

Correspondence:

Yoshiaki Nishioka, M.D. and Katsushige Abe, M.D. and Ph.D.

Second Department of Internal Medicine

Nagasaki University School of Medicine

1-7-1 Sakamoto, Nagasaki 852-8501, Japan

Phone: +81-95-849-7282

FAX: +81-95-849-7285

e-mail: yyynnn@vc.fctv-net.jp (Yoshiaki Nishioka, M.D.)

rukonyan@ga2.so-net.ne.jp (Katsushige Abe, M.D.)

Abstract

Background. Patients on long-term peritoneal dialysis develop progressive peritoneal fibrosis and loss of mesothelial layer. Regeneration of the mesothelium has been reported in the normal peritoneum, but not in the fibrotic peritoneum. Moreover, the origin of the regenerated mesothelial cells remains obscure. The aim of this study was to investigate mesothelial regeneration in fibrotic peritoneum induced by chlorhexidine gluconate.

Methods. Peritoneal fibrosis was induced by injection of CG into the peritoneal cavity of Wistar rats. After injection, the abdomen was opened, and the parietal fibrotic peritoneum with mesothelial cells was stripped from the abdominal wall, and then the abdominal incision was closed. Rats were sacrificed and peritoneal tissues were dissected out at 0, 1, 3, 5, or 7 days after the stripping procedure.

Results. Spindle-shaped cells with microvilli appeared on the surface of stripped peritoneum at day 3 after denudation. Immunohistochemistry identified staining for vimentin, a marker of mesoderm cells, in the spindle-shaped cells at days 3, 5, and 7. Expression of α -SMA was observed in the same cells at days 3 and 5, but not 7. Expression of cytokeratin and HBME-1, markers for mesothelial cells, in these cells was delayed until day 7.

Conclusions. Mesothelium can regenerate on the fibrotic peritoneum. The regenerated mesothelial cells seem to originate from vimentin-positive mesenchymal cells.

Key words: mesothelial cells, peritoneal fibrosis, mesenchymal cells, regeneration, mesenchymal-epithelial transition

Introduction

The peritoneal membrane is lined with a monolayer of mesothelial cells, which act as a permeability barrier. In fact, these cells secrete various substances that are involved in the regulation of peritoneal permeability and local host defense [1, 2]. However, it is well known that long-term peritoneal dialysis (PD) causes chronic morphological changes in the peritoneum, which progressively becomes denuded of mesothelial cells and fibrotic with increased submesothelial collagen deposition [2-4]. Therefore, reconstruction of the mesothelium is essential for a better prognosis of patients on longer PD.

Several studies have reported that the peritoneum including the lining mesothelial cells can regenerate [5-16]. To our knowledge, the first observation of mesothelial regeneration on the peritoneum was reported in 1955, using light microscopy [5], and more detailed observation by scanning electron microscopy (SEM) was reported in 1966 [8]. In the previous studies, the peritoneum was removed from the abdominal wall by various procedures, such as excision [5-8,11-14], inflicting burn or cold wounds [8,15,16], attaching and peeling a thin dry film of gelatin [9], drying with a stream of air [10], and the regeneration of the peritoneum in the denuded area. Unfortunately, however, the regeneration of the mesothelium had been examined in these previous reports using normal peritoneum only devoid of fibrosis. To our knowledge, there is no information on mesothelial regeneration on fibrotic peritoneum, and there is little or no information on the source of mesothelial cells that participate in the reconstruction of the mesothelium.

The present study was designed to examine the possible regeneration of the mesothelial layer in the fibrotic peritoneum, and the process that controls such regeneration. For this purpose, we first induced chemical fibrosis of the peritoneum experimentally by applying chlorhexidine gluconate (CG) into the peritoneal cavity of rats [17-19], and then examined the morphological and immunohistochemical changes.

Materials and Methods

Animals

Twenty-five male Wistar rats (8 weeks of age, about 250 g body weight) were used in this study. They were housed in a light- and temperature-controlled room in the Biomedical Research Center, Center for Frontier Life Sciences, Nagasaki University. They had free access to laboratory chow and tap water in standard rodent cages. The experimental protocol was inspected by Animal Care and Use Committee of Nagasaki University School, and approved by the President of Nagasaki University.

Treatment with chlorhexidine gluconate and tissue preparation

Peritoneal fibrosis was induced by intraperitoneal injection of 0.1% CG in 15% ethanol dissolved in saline, as described previously with slight modification [17-19]. Briefly, under ether anesthesia, rats received a daily intraperitoneal injection of CG at a volume of 10 mL/kg body weight over a period of 14 days. To avoid direct damage of the peritoneum by repeated injections, injections were made at the lower part of the peritoneum. In this model, the thickness of the peritoneum was increased at 7 days after the first injection [17]. Seven days after the final CG injection, the rat was anesthetized and the abdomen opened through a long midline incision and 3 cm x 4 cm square wound was made by the stripping procedure. In the Stripping procedure, the parietal fibrotic peritoneum was anchored with forceps and the fibrotic peritoneum with mesothelial cells was removed by stripping the surface of peritoneum several

times with the other forceps in the square, keeping marks on the four corners to allow us recognize the stripped area, then closed the abdominal incision. At 0, 1, 3, 5, or 7 days after the stripping procedure, five rats were sacrificed at each time point and the peritoneum including the stripped area was dissected carefully. The obtained tissues were fixed with 4% paraformaldehyde in phosphate buffered saline (PBS) for 72 h immediately after excision and embedded in paraffin, or were fixed immediately with 2.5% glutaraldehyde in 0.1 M sodium cacodylate containing 2 mM CaCl_2 (cacodylate buffer) for 60 min. For histopathological examination, paraffin-embedded tissue sections (4- μm thick) were stained with hematoxylin and eosin (H&E).

Immunohistochemistry

Paraffin-embedded tissue sections (4 μm thick) were used for immunohistochemically, as described previously [17-19]. Briefly, deparaffinized tissue sections were incubated for 30 minutes with a blocking buffer containing 10% normal goat serum, 10% normal swine serum and 10% fetal calf serum (FCS) in PBS. The sections were then reacted for 1 hour with the following primary monoclonal antibodies, which were diluted in the blocking buffer; anti-mouse ED-1 diluted 1/100 as a marker for macrophages (Serotec, Oxford, UK); anti- vimentin diluted 1/75 as a marker for mesenchymal cells (M0725, Dako, Glostrup, Denmark); anti- α -smooth muscle actin (α -SMA) diluted 1/100 as a marker for myofibroblasts (M0851, Dako); anti-cytokeratin diluted 1/50 as a marker for mesothelial cells (M0821, Dako); anti-HBME-1 diluted 1/50 as a marker for mesothelial cells [20-22] (M3505, Dako). After reacting with the primary antibodies, with the exception of anti-cytokeratin antibody, the sections were reacted

for 30 minutes with the following antibodies diluted with the blocking buffer; horseradish peroxidase (HRP)-conjugated rabbit anti-mouse antibody diluted 1/100 (P260, Dako) and HRP-conjugated swine anti-rabbit antibody (P399, Dako). The sections reacted with anti-cytokeratin antibody was stained by the streptavidin-biotin-peroxidase complex kit (LSAB2/HRP kit, Dako). The sites of HRP were visualized with H₂O₂ and 3-3 diaminobenzidine tetrahydrochloride. Finally, the sections were counterstained with methyl green and mounted. For all specimens, negative control studies were performed by using irrelevant immunoglobulins (Ig) of subclasses similar to those of the primary antibodies, such as nonspecific mouse IgG1 (X931, Dako), IgG2 (X943, Dako), and rabbit IgG (X903, Dako), instead of the primary antibodies. No positively-stained cells were identified in the negative control sections (data not shown).

In order to detect both HBME-1 and vimentin simultaneously in the same section, double staining was performed. For HBME-1 staining, sections were reacted with a complex of anti-HBME-1 antibody and HRP-conjugated rabbit anti-mouse antibody and reaction products were visualized as described above. After staining HBME-1, the sections were washed with PBS to stop the color reaction. Sections were then incubated for 90 minutes at room temperature with a blocking solution and reacted with a complex of antibody for vimentin and HRP-conjugated goat anti mouse antibody. A second chromogen, True Blue (71-00-64; KPL, Gaithersburg, Maryland, USA) was then applied, resulting in the staining of positive cells in blue. The tissue sections were not counterstained with methyl green, since this counterstaining might have interfered with the color from chromogen.

Electron microscopy

After washing with cacodylate buffer, the specimens were postfixed in cold 1% OsO₄ in the same buffer for 30 min, and then stained with 2% uranyl acetate for 30 min. The specimens were dehydrated in a critical point apparatus, and examined with a JSM 6700 F scanning electron microscope (SEM) (JEOL, Japan), after a gold sputter coating.

Results

Histological examination

Morphological changes were assessed by H&E staining. In CG treated rats, the peritoneum was seriously thickened and some mesothelial cells were identified on the surface of the peritoneum with submesothelial fibrosis (Figs. 1A and 2A), while no cells were observed at day 0 on the surface of the stripped peritoneal area (Figs. 1B and 2B). After day 3, the peritoneum was thickened and surrounded by several cells in the stripped pieces (Fig. 1D, E, F). As shown in Figure 2, the surface of the stripped area was markedly changed: the surface of the stripped peritoneum was covered by round-shaped cells at day 1 (Fig. 2C), and by spindle-shaped cells at day 3, and then these cells gradually flattened on the surface (Fig. 2D, E, F). The healing process was very similar in each rat and no variation was observed in this experiment.

Electron microscopic examination

Figures 3 and 4 show the surface of the stripped peritoneum by SEM. The surface was completely devoid of mesothelial cells at day 0 (Fig. 3A). The higher magnification image of SEM showed covering of the surface with fibrous elements without mesothelial cells just after the stripping procedure (Fig. 4A). At day 1, the peritoneal surface was covered with strands of fibrin and a number of round-shaped cells were observed on the fibrin. (Fig. 3B and 4B). These cells had long and slender filopodia extending from one cell to another and to the substratum. The number of spindle shaped cells was very few on the fibrin at day 1. At day 3, the most prominent

changes were noted; the number of round-shaped cells decreased markedly (Fig. 3C) and the surface was covered by spindle-shaped cells. The morphology of these cells was obviously different from the round-shaped cells seen at day 1, and these spindle-shaped cells had short microvilli (Fig. 4C). After day 3, most of the cells on the surface of peritoneum was replaced and covered by spindle shaped cells. At day 5, the number and length of these microvilli increased (Fig. 4D). At day 7, the surface of these cells was covered with many fine microvilli (Fig. 4E).

Immunohistochemistry

To identify the types of cells present on the surface of the stripped peritoneum, we performed immunohistochemistry for ED-1, a marker of macrophages, and vimentin, a marker of mesenchymal cells, and α -smooth muscle actin (α -SMA), a marker of myofibroblasts. We also performed immunohistochemistry for cytokeratin and HBME-1, a marker of mesothelial cells [20-22].

Expression of ED-1. ED-1-positive cells were abundantly present on the surface cells of the stripped peritoneum at day 1 (Fig. 5A). However, at day 3, the number of round-shaped cells positive to ED-1 decreased, and the surface became covered with many ED-1 negative cells (Fig. 5B). After days 5 and 7, only spindle-shaped cells, which were ED-1-negative, were on the surface, while ED-1-positive cells were observed under the surface of stripped peritoneum (Fig. 5C, D).

Expression of vimentin. There were no vimentin-positive cells at day 1 (Fig. 6A). Staining for vimentin was observed in the spindle shaped cells on the surface of the peritoneum at days 3, 5, and 7 (Fig. 6B, C, D). However, vimentin staining was not observed in the round-shaped cells on the surface at day 3 (Fig. 6B; arrowheads).

Expression of α -SMA. There were no α -SMA-positive cells at day 1 (Fig. 7A). Expression of α -SMA was observed in spindle-shaped cells on the surface of the peritoneum at days 3 and 5 (Fig. 7B, C), but disappeared at day 7 (Fig. 7D; arrowheads).

Expression of cytokeratin and HBME-1. Expression of cytokeratin was not observed on the surface spindle cells of the stripped peritoneum at days 1, 3, and 5 (Fig. 8A, B, C), but appeared only at day 7 (Fig. 8D). Similarly, no staining for HBME-1 was found at days 1, 3, and 5 (Fig. 9A, B, C), while a strong staining was detected at day 7 (Fig. 9D).

To determine whether HBME-1 positive cells were originated from vimentin positive cells, we performed double staining for HBME-1 and vimentin in the same section. The staining revealed that the cells positive for HBME-1 (brown) were stained for vimentin (blue) on the surface of peritoneum at day 7 (Fig. 10).

Discussion

Peritoneal dialysis is essential in renal replacement therapy. However, the peritoneum of patients undergoing long-term PD shows loss of the mesothelial cell layer and peritoneal fibrosis, which might ultimately cause functional failure of the peritoneal membrane [2-4]. Therefore, for effective long-term PD, peritoneal regeneration is clinically important, as is the reconstruction mechanism of fibrotic peritoneal tissue and replacement of mesothelial cells by mesothelial cells. Previous studies have demonstrated the regeneration of peritoneum in normal adult rats by using the various procedures to remove the peritoneum, such as excision, burning wound and mechanical wounds with forceps. These studies showed that all peritoneal defects were covered by surface layer of flattened cells morphologically resemble to mesothelial cells within 5 days and 10 days after peritoneal removal procedures, new mesothelium was histologically indistinguishable from normal peritoneum. In the present study, we identified a clear regeneration of the mesothelial cell layer on the fibrotic peritoneum and healing process in fibrotic peritoneum was very similar to that in normal peritoneum. The replaced cells had microvilli, the most important feature of the mesothelium under the SEM, and were confirmed to be mesothelial cells as determined by the expression of cytokeratin and HBME-1. Although this model does not completely mimic human disease, and the process of denuding mesothelial cells is surgical removal, confirmation of mesothelial cell layer regeneration on the fibrotic peritoneum is important.

Our results indicate that mesenchymal cells could change to mesothelial cells during the process of peritoneal regeneration. A recent study indicated that the balance between epithelial-mesenchymal transition (EMT) and mesenchymal-epithelial transition (MET) is essential for progression and repair of fibrosis [23]. In peritoneal fibrosis, Yáñez-Mó et al. [24] reported that EMT was also observed in an *in vitro* study of the peritoneum from patients with peritoneal dialysis. They reported the identification of fibroblast-like mesothelial cells positive for cytokeratin in fibrotic peritoneum from patients on long-term PD, suggesting the involvement of EMT in the progression of peritoneal fibrosis. Although we did not perform immunoelectron microscopic examination in the present study or *in vitro* study, the finding of cells positive for markers of mesenchymal cells on the surface provide support for the role of MET in mesothelial regeneration. In fact, Amari et al. [25] used immunohistochemistry and electron microscopy to show conversion of cultured fibroblasts, obtained from the parietal pleura of rats, to mesothelial cells.

Before the appearance of vimentin-positive cells, ED-1-positive cells were observed on the surface of the regenerating peritoneum. SEM showed that these cells had filopodia, which are known as a main feature of macrophages (Fig. 4B). Previous reports also showed that the process of mesothelial healing began with the appearance of round, macrophage-like cells [6-10, 12-16]. Two interpretations had been proposed for the relationship between macrophages and mesothelial cells. Ellis *et al.* [6], Raftery [12], and Whitaker *et al.* [15] proposed that macrophages on the peritoneal surface were ultimately replaced by cells that differentiated into mesothelial cells. On the other hand, Eskland [7] and Ryan *et al.* [10] hypothesized that the

macrophage-like cells gradually transform into mesothelial cells. Clearly, our results demonstrating that vimentin-positive cells are different from ED-1-positive cells (Fig. 6B) favored the former hypothesis.

In conclusion, we demonstrated in the present study that mesenchymal cells expressing vimentin appeared before mesothelial regeneration on the fibrotic peritoneum. Our results suggest that MET is associated with the regeneration of peritoneal mesothelium. The precise molecular mechanisms that trigger, propagate and terminate peritoneal regeneration require further investigation.

References

1. Brulez HF, Verbrugh HA. First-line defense mechanisms in the peritoneal cavity during peritoneal dialysis. *Perit Dial Int.* 1995;15 Suppl:S24-S33.
2. Kerdiet RT. The peritoneal membrane in chronic peritoneal dialysis patients. *Kidney Int.* 1999;55:341-356.
3. Gandhi VC, Humayun HM, Ing TS, et al. Sclerotic thickening of the peritoneal membrane in maintenance peritoneal dialysis patients. *Arch Intern Med.* 1980;140:1201-1203.
4. Williams JD, Craig KJ, Topley N, et al. Peritoneal Biopsy Study Group: Morphologic changes in the peritoneal membrane of patients with renal disease. *J Am Soc Nephrol.* 2002;13:470-479.
5. Williams DC. The peritoneum. A plea for a change in attitude towards this membrane. *Br J Surg.* 1955;42:401-405.
6. Ellis H, Harrison W, Hugh TB. The healing of peritoneum under normal and pathological conditions. *Br J Surg.* 1965;52:471-476.
7. Eskeland G. Regeneration of parietal peritoneum in rats. 1. A light microscopic study. *Acta Pathol Microbiol Scand.* 1966;68:355-378.
8. Eskeland G, Kjaerheim A. Regeneration of parietal peritoneum in rats. 2. An electron microscopic study. *Acta Pathol Microbiol Scand.* 1966;68:379-395.
9. Watters WB, Buck RC. Scanning electron microscopy of mesothelial regeneration in the rat. *Lab Invest.* 1972;26:604-609.

10. Ryan MB, Grobety J, Majno G. Mesothelial injury and recovery. *Am J Pathol.* 1973;71:93-102
11. Raftery AT. Regeneration of parietal and visceral peritoneum in the immature animals: a light and electron microscopical study. *Br J Surg.* 1973;60:969-975
12. Raftery AT. Regeneration of parietal and visceral peritoneum: an electron microscopical study. *J Anat.* 1973;115:375-392.
13. Raftery AT. Regeneration of parietal and visceral peritoneum: an enzyme histochemical study. *J Anat.* 1976;121:589-597.
14. Raftery AT. Regeneration of peritoneum: fibrinolytic study. *J Anat.* 1976;129:659-664.
15. Whitaker D, Papadimitriou J. Mesothelial healing: morphological and kinetic investigations. *J Pathol.* 1985;145:159-175.
16. Mutsaers SE, Whitaker D, Papadimitriou J. Mesothelial regeneration is not dependent on subserosal cells. *J Pathol.* 2000;190:86-92.
17. Mishima Y, Miyazaki M, Abe K, et al. Enhanced expression of heat shock protein 47 in rat model of peritoneal fibrosis. *Perit Dial Int.* 2003;23:14-22.
18. Nishino T, Miyazaki M, Abe K, et al. Antisense oligonucleotides against collagen-binding stress protein HSP47 suppress peritoneal fibrosis in rat. *Kidney Int.* 2003;64:887-896.
19. Yoshio Y, Miyazaki M, Abe K, et al. TNP-470, an angiogenesis inhibitor, suppress the progression of peritoneal fibrosis in mouse experimental model. *Kidney Int.* 2004;66:1677-1685.

20. Sheibani K, Esteban JM, Bailey A, Battifora H, Weiss LM. Immunopathologic and molecular studies as an aid to the diagnosis of malignant mesothelioma. *Hum Pathol.* 1992;23:107-116.
21. Miettinen M, Kovatich AJ. HBME-1 a monoclonal antibody useful in the differential diagnosis of mesothelioma, adenocarcinoma, and soft-tissue and bone tumors. *Appl Immunohistochem.* 1995;3:115-122.
22. Fetsch PA, Simsir A, Abati A. Comparison of antibodies to HBME-1 and calretinin for the detection of mesothelial cells in effusion cytology. *Diagn Cytopathol.* 2001;25:158-161.
23. Neilson EG. Mechanism of disease: fibroblasts-a new look at an old problem. *Nat Clin Pract Nephrol.* 2006;2:101-108.
24. Yáñez-Mó M, Lara-Pezzi E, Selgas R, et al. Peritoneal dialysis and epithelial-to-mesenchymal transition of mesothelial cells. *N Engl J Med.* 2003;348:403-413.
25. Amari M, Taguchi K, Iwahara M, Shibuya K, Naoe S. Immunohistochemical and ultrastructural study on effect of fibroblast growth factor on transformation of fibroblasts to regenerated mesothelial cells. *Med Electron Microsc.* 2002;35:225-233.

Legends of Figures

Figure 1. Hematoxylin and eosin staining of the stripped peritoneum.

(A) Significant thickening of the peritoneum was noted in CG injected rats. (B) Collagen fibers appeared over the abdominal muscles immediately following the stripping procedure at day 0. (C) No thickening of peritoneum was observed at day 1. (D) Thickening of peritoneum was observed at day 3. (E) Thickening of the peritoneum increased and cells accumulated above the middle of the peritoneum at day 5. (F) Cells were uniformly scattered in peritoneum at day 7. Magnification $\times 100$.

Figure 2. Hematoxylin and eosin staining of the surface of stripped peritoneum

(A) Some mesothelial cells are on the surface of thickened peritoneum in CG injected rats. (B) The monolayer of mesothelial cells disappeared on the surface immediately following the stripping procedure at day 0. (C) Some round-shaped cells appeared on the surface at day 1. (D) Round shaped cells markedly decreased in number and the surface was covered with spindle-shaped cells at day 3. (E) The latter cells showed more spindling at days 5 and 7 (F). Magnification $\times 400$.

Figure 3. Scanning electron microscopy of the surface of the stripped peritoneum.

(A) Note lack of cells over the surface immediately following the stripping procedure at day 0. (B) Scattered round-shaped cells over the surface at day 1. (C) At day 3, the surface was covered with spindle-shaped cells, which clearly differed from the cells at

day 1. (D) The spindle-shaped cells junction on the surface became tight at day 5, and loose again at day 7 (E).

Figure 4. Scanning electron microscopy of the surface of the stripped peritoneum (higher magnification of Figure 3).

(A) Fibrous tissue covered the surface without mesothelial cells immediately following the stripping procedure at day 0. (B) The surface of the peritoneum was covered with strands of fibrin and several round shaped cells were observed on the fibrin at day 1. These cells had long and slender filopodia (arrowheads). (C) Large spindle-shaped cells over the surface and these cells had short microvilli. (D) These microvilli increased and became long at days 5 and 7 (E).

Figure 5. Immunohistochemistry for ED-1.

(A) ED-1-positive cells were abundantly present on the surface cells of stripped peritoneum at day 1. (B) ED-1-positive cells decreased in number and the surface became covered with many ED-1-negative cells at day 3 (arrowheads). (C) No ED-1-positive cells were identified on the surface at days 5 and 7 (D). Magnification $\times 400$.

Figure 6. Immunohistochemistry for vimentin.

(A) No vimentin-positive cells were identified at day 1. (B) Staining for vimentin was observed in spindle-shaped cells on the surface at days 3, 5 (C) and 7 (D). Vimentin

staining was not observed in the round-shaped cells on the surface at day 3 (B; arrowheads). Magnification $\times 400$.

Figure 7. Immunohistochemistry for α -SMA.

(A) No α -SMA-positive cells were detected at day 1. (B) Expression of α -SMA was noted in cells on the surface at days 3, and 5 (C). (D) No α -SMA expression was observed in cells on the surface at day 7 (arrowheads). Magnification $\times 400$.

Figure 8. Immunohistochemistry for cytokeratin.

(A) Expression of cytokeratin was negative in cells identified on the surface at day 1, day 3 (B), and day 5 (C). (D) Expression of cytokeratin was observed in cells on the surface at day 7. Magnification $\times 400$.

Figure 9. Immunohistochemistry for HBME-1.

(A) Expression of HBME-1 was negative in cells identified on the surface at day 1, day 3 (B), and day 5 (C). (D) Expression of HBME-1 was observed in cells on the surface at day 7. Magnification $\times 400$.

Figure 10. Double staining for HBME-1 and vimentin in the same sections.

Note that HBME-1 positive cells (brown) on the surface of peritoneum are also positive for vimentin (blue; arrowheads). Magnification $\times 400$.

Figure 1. Hematoxylin and Eosin staining of peritoneum

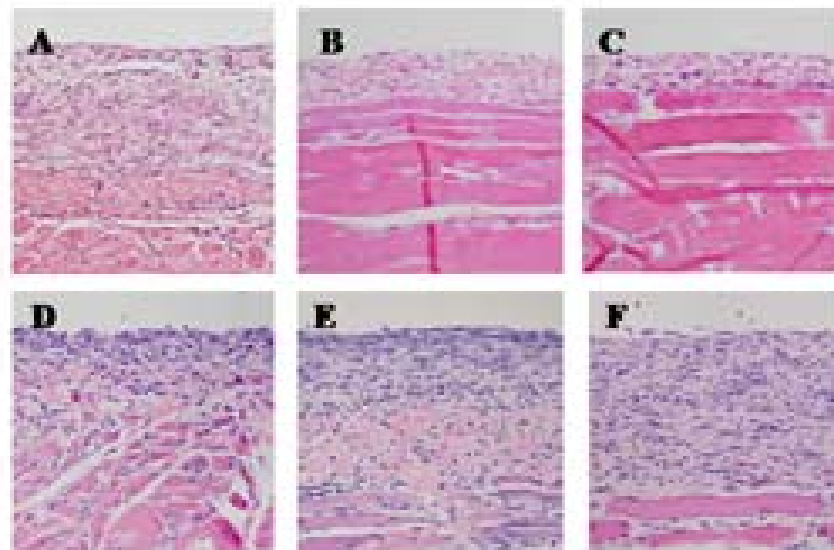


Figure 2. Hematoxylin and Eosin staining of peritoneum

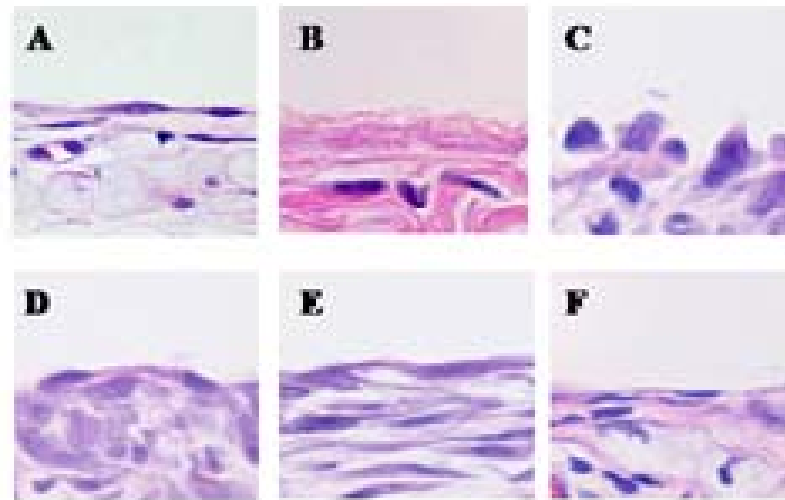


Figure 3. SEM examinations of the surface of the stripped peritoneum

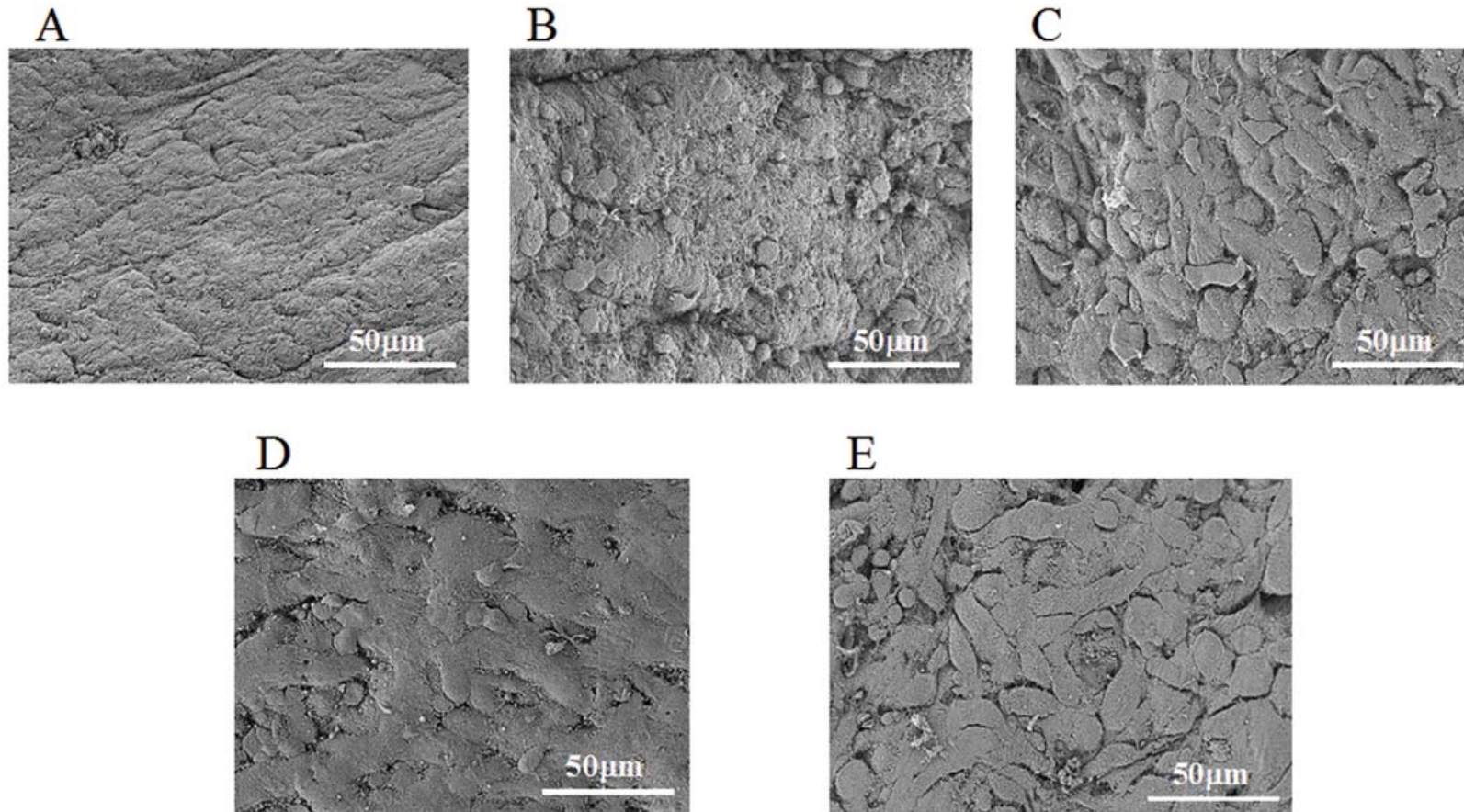


Figure 4. SEM examinations of the surface of the stripped peritoneum

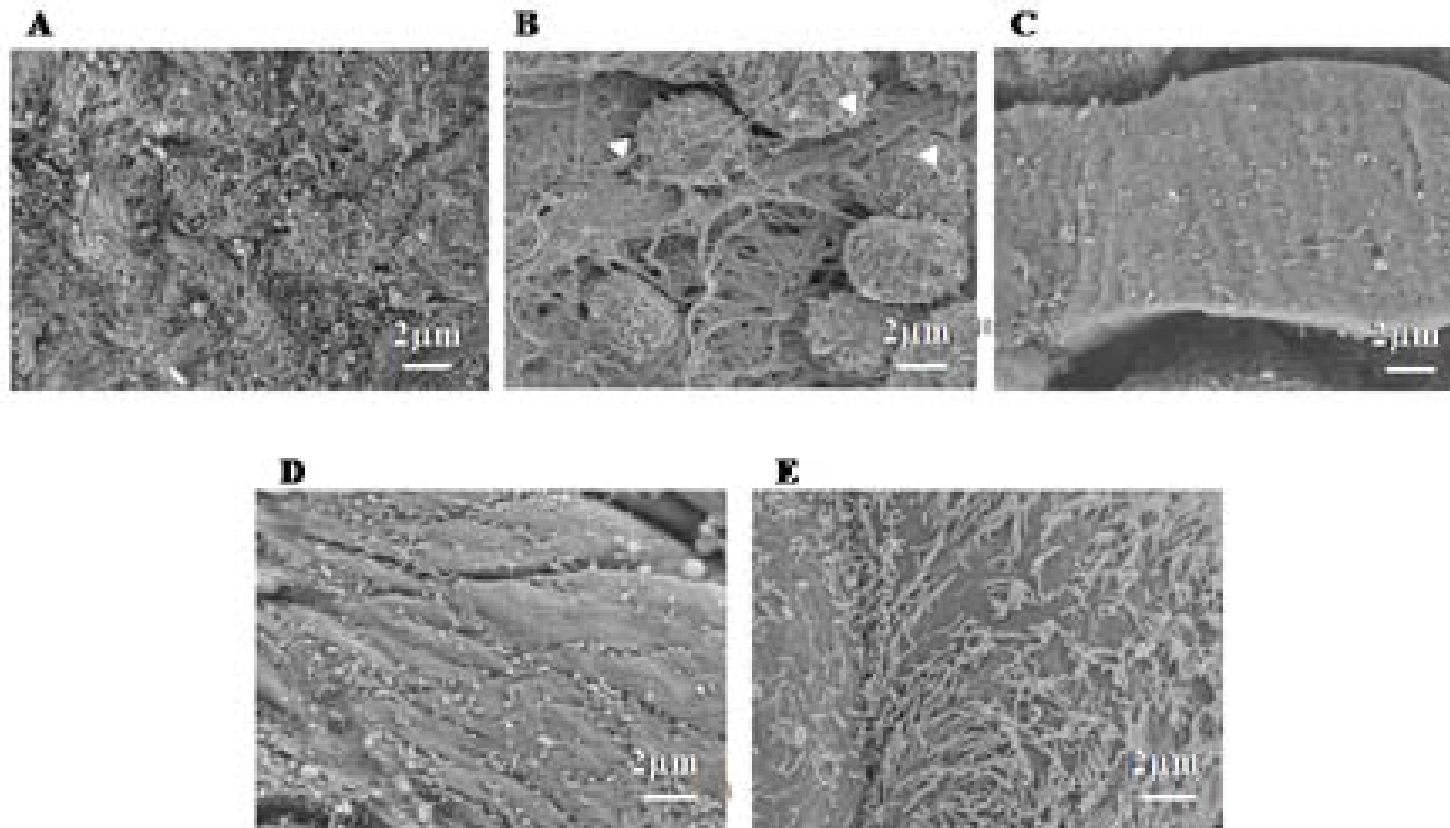


Figure 5. Immunohistochemistry for ED-1

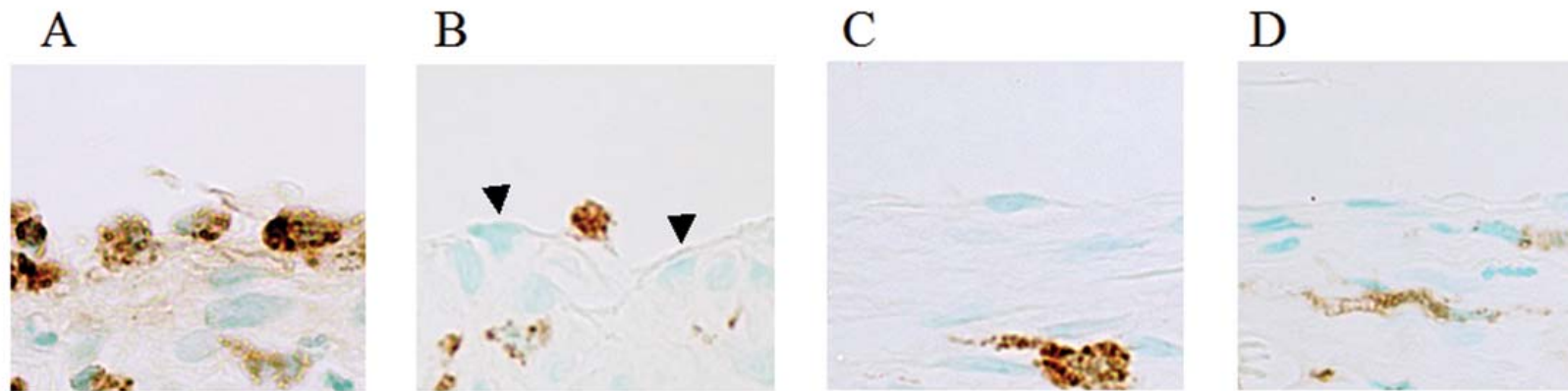


Figure 6. Immunohistochemistry for vimentin

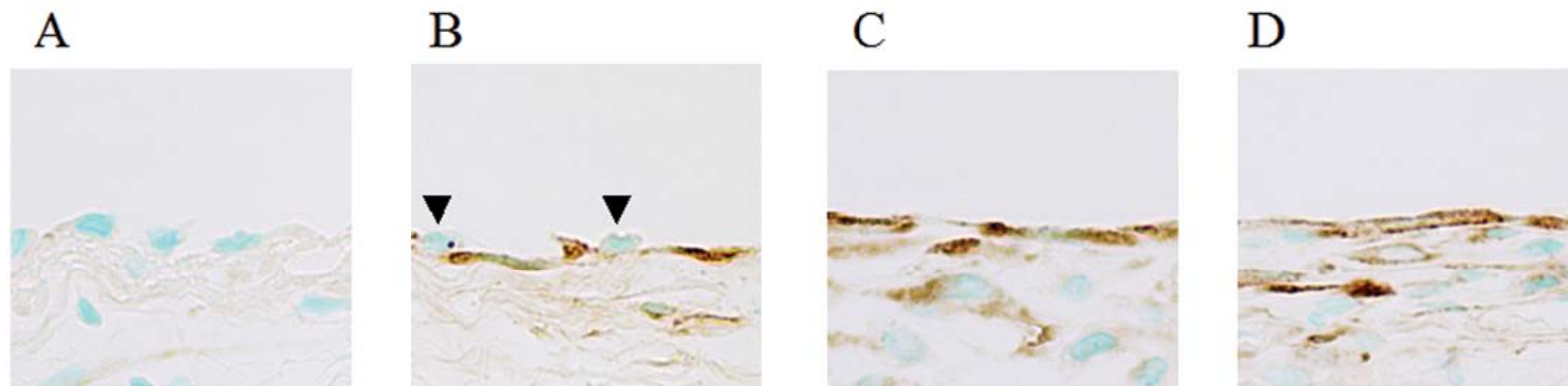


Figure 7. Immunohistochemistry for α -SMA

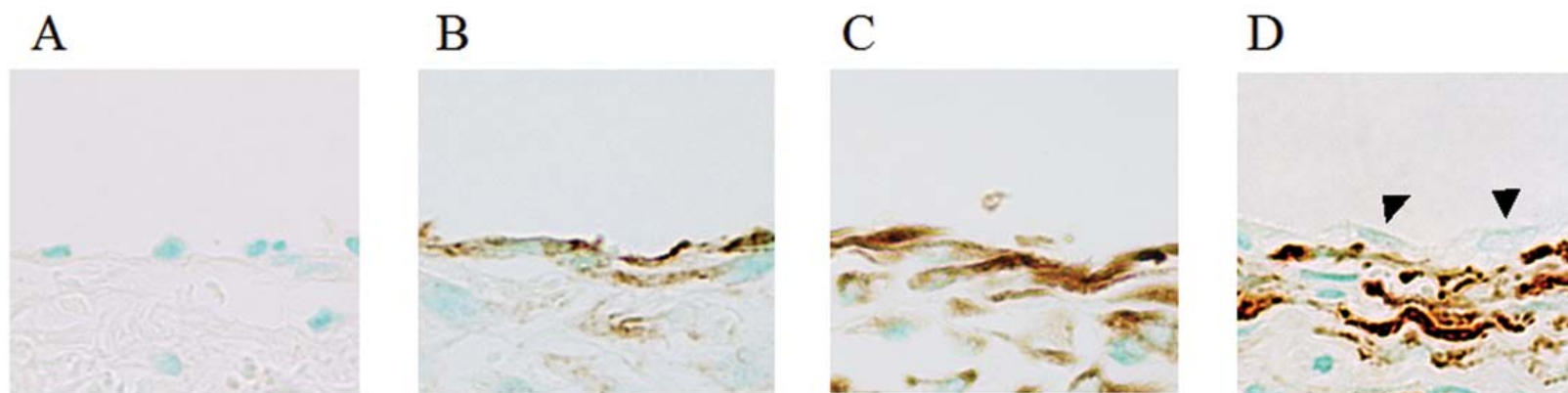


Figure 8. Immunohistochemistry for cytokeratin

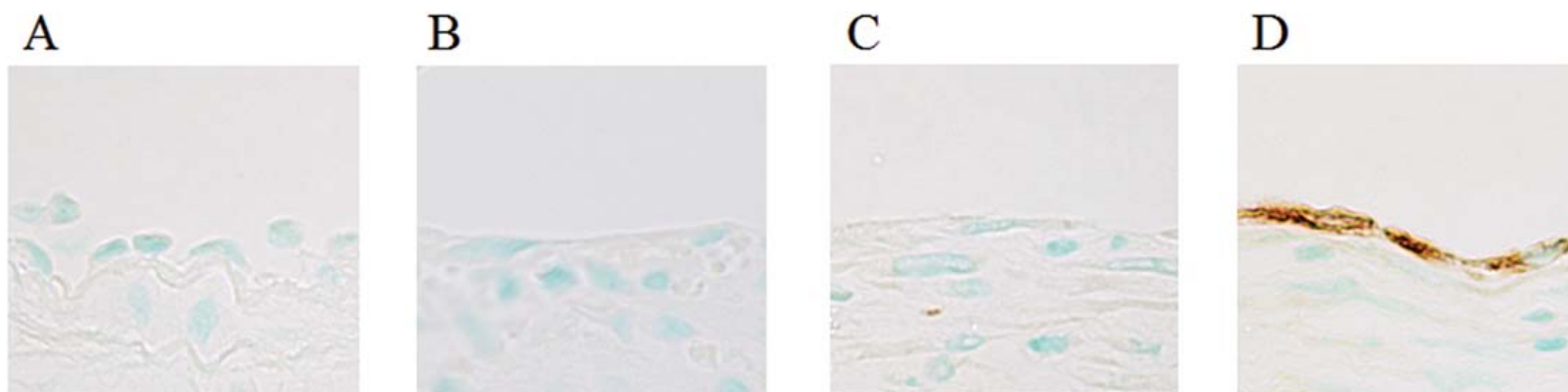


Figure 9 . Immunohistochemistry for HBME-1

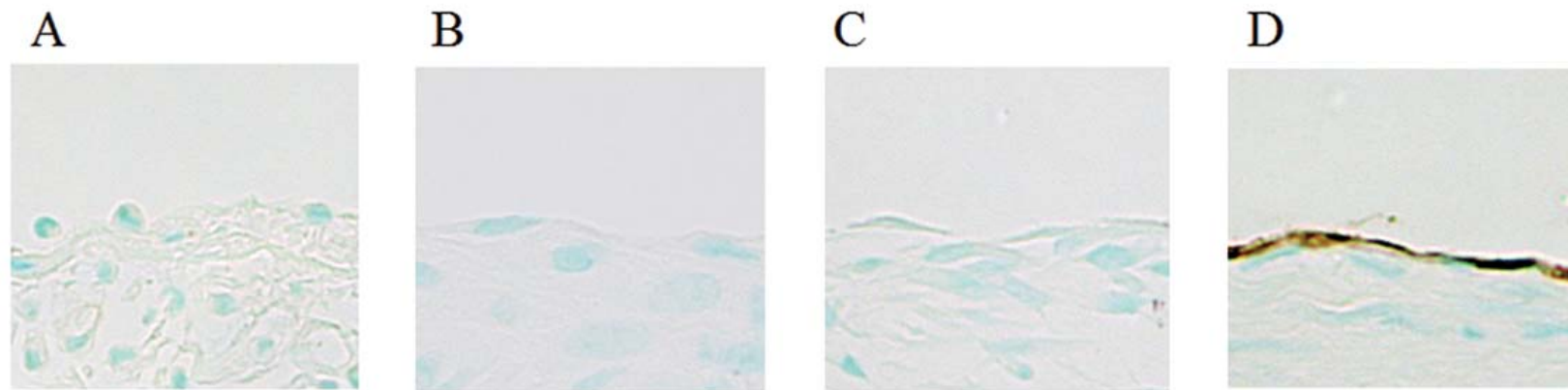


Figure 10.
Double staining for HBME-1 and vimentin in the same sections

